PHYSICAL REVIEW B VOLUME 23, NUMBER 10 15 MAY 1981

# Semiconductor-metal transition in doped polyacetylene

Eugene J. Mele and Michael J. Rice
*Xerox Webster Research Center, Webster, New York 14580*
(Received 16 October 1980)

We present studies of the stability and electronic structure of doped finite model polyenes as a function of dopant concentration. The results illustrate the nature of semiconductor-metal transition in doped polyacetylene which differs qualitatively from an impurity-band insulator-metal transition in a conventional semiconductor. The evolution from insulating behavior to metallic behavior is characterized by four regimes: (I) accommodation of excess carriers in solitons pinned at impurity sites at low dopant concentration, (II) formation of isolated quasimetallic regions resulting from statistical fluctuations in dopant density at slightly higher concentrations, (III) formation of a dense band of localized states resulting from the disordering of an incommensurate charge density wave in the random field of the ionized impurities at still higher concentrations, and (IV) suppression of bond alternation in the presence of strong disorder due to a dense distribution of impurities at extremely high concentrations. The insulator-metal transition occurs at the onset of regime III, and is found at a $\sim 10$ at. % dopant concentration in a strictly one-dimensional theory. Including three-dimensional interchain coupling the density is expected to be reduced below 5% where it is observed experimentally. Direct probes of the Fermi level state density are expected to show a smooth evolution through the transition region due to statistical fluctuations in the local dopant density.

## I. INTRODUCTION

Polyacetylene, long known to synthetic chemists as a black amorphous powder, has recently undergone a renaissance of interest among solid-state researchers. This revival follows the successful synthesis of the material into self-supporting films[1,2] and the subsequent observations of profoundly altered electrical properties upon doping with a variety of donors and acceptors.[3,4] Superficially, the behavior of polyacetylene upon doping appears rather similar to that of a conventional semiconductor; i.e., a pristine insulator shows semiconducting properties when lightly doped.[3-6] and undergoes an insulator-metal transition[3] at high doping levels. Upon closer consideration, however, it becomes apparent that the behavior of polyacetylene upon doping is qualitatively different from that of a conventional crystalline semiconductor. The $\pi$-electron manifold in $(CH)_x$ is a quasi-one-dimensional electron gas, with an estimated bandwidth parallel to the chain axis exceeding the interchain bandwidth by nearly 2 orders of magnitude.[7] Such a system is susceptible to a variety of electronic and/or structural instabilities[8-17]; in the work that follows we focus on the Peierls instability, which provides a convenient and familiar framework with which to interpret bond alternation, which is observed to occur in neutral long chain polyenes[18] and is anticipated to persist in the (infinite) polyacetylene limit.[8,9,12,15] That is, the elastic energy required to deform the system from a uniform bond length structure is overcome by the tendency of the electron gas to form relatively weak $\pi$ bonds in half the bonds on the chain, transforming the infinite polyene from a paramagnetic conducting structure to a diamagnetic insulating one. Upon addition of a few carriers to the chain, such an argument predicts that the chain will again seek a diamagnetic insulating ground state. Physically this is manifested by the trapping of added carriers in solitons,[19-22] discommensurations in the bond alternation which reverse the magnitude of the bond alternation (i.e., the order in which the bonds alternate). Each of these defects produces a half-filled midgap level when neutral, and accommodates an excess carrier in a diamagnetic center in the charged polyene. This theoretical expectation is borne out in a number of experimental studies of the magnetic character[23,24] of and the low-lying electronic excitations from[25] the doped ground state, and vibrational excitations of such kinks have even been observed.[26,27] Such behavior contrasts markedly with the behavior of a substitutionally doped crystalline group-IV semiconductor in which defect formation in response to an excess carrier is strongly inhibited by the constrained geometry of a three-dimensional covalently bonded network. In fact, behavior similar in spirit to that observed in $(CH)_x$ is presumed to occur in doped trigonal Se where this structural constraint is relaxed.[28]

In this paper we examine the behavior of the polyene at higher doping levels and follow the implications of a Peierls model through the semiconductor-metal transition in polyacetylene.[29] We find a semiconductor-metal transition in this system which differs markedly from an impurity-band insulator-metal transition in a conventional

semiconductor.[30] We find that the polyene as described by an ideal Peierls model shows a strong tendency to seek an insulating ground state, even for deviations in band filling from the half-filled band exceeding 14%, i.e., well past the observed insulator-metal transition. Upon closer study we note that this tendency to form an incommensurate insulating structure is strongly suppressed by interactions between the polyene $\pi$ electrons and impurity sites randomly situated adjacent to the chain. This interaction, which is treated alternately by models in which the impurities interact via a screened Coulomb interaction or via direct hybridization with nearby $\pi$ orbitals, strongly structurally disorders the ideal incommensurate lattice and leads to a semiconductor-metal transition near the 10 at.% doping level. This transition density is further suppressed by interchain coupling in this quasi-one-dimensional system, and including such effects the transition density is suppressed below 5% where it is observed experimentally. We find that the metallic structure which occurs just above this threshold is characterized by a nonzero order parameter, i.e., bond alternation persists into the metallic state, stabilized by a pseudogap in the density of states. At still higher impurity concentrations, a further structural transformation occurs where bond alternation becomes strongly suppressed as well.

As will become apparent, the semiconductor-metal transition in this material is a collective process involving all the $\pi$ electrons in the system, not merely the extrinsic carriers. Since the number of added carriers required to seed this process locally is quite low, we expect statistical fluctuations in the local dopant density to be very significant. Consequently, most macroscopic experimental probes of the metallic character of this system are expected to show a smooth evolution through the "transition" as microscopic quasi metallic regions flourish. This seems to be in general accord with most of the experimental information reported on this system to date.

In this paper we will proceed as follows. In Sec. II we present the mechanics of the studies, specifying the Hamiltonian we employ and the numerical techniques which are used in these calculations. The reader who is merely interested in the results of these calculations is advised to inspect the trial functions we describe in Sec. IIC and then pass to Sec. III where we discuss the results of calculations on ideal incommensurate structures. In Sec. IV we consider the effects of the ionized impurities and three-dimensional coupling in this system and amend our Hamiltonian to include these effects. In Sec. V we examine the effects of these perturbations on the ideal incommensurate structures, and in Sec. VI we show the emergence of an insulator-metal transition due to the rancom potential. In Sec. VII we consider the role of statistical fluctuations in the dopant concentration and discuss some experimental implications of the model. A synopsis is given in Sec. VIII.

## II. THEORETICAL FORMULATION

### A. Hamiltonian

To study the coupling of the $\pi$ electrons to lattice displacements in the polyene, we adopt an idealized Hamiltonian for a linear chain:

$$H = \sum (t_{n+1,n} c^{\dagger}_{n,\sigma} c_{n+1,\sigma} + \text{H.c.}) + \tfrac{1}{2} \sum K(u_{n+1} - u_n)^2 + \sum (M/2)\dot{u}_n^2 - \sum \Gamma(u_{n+1} - u_n) . \quad (1)$$

Here $c_{n,\sigma}$ annihilates a $\pi$ electron of spin $\sigma$ on site $n$, $u_n$ labels the longitudinal displacement of the $n$th site from its position in an ideal undistorted metallic chain and $M$ is the CH mass. The $\{t_{ij}\}$ define a set of nearest-neighbor hopping integrals which depend parametrically on the displacement $\{u_n\}$:

$$t_{n+1,n} = t_0 - \alpha[(u_{n+1} - u_n)] . \quad (2)$$

The final term in Eq. (1) is a repulsive energy, *linear* in the atomic displacements, which is required to stabilize a finite chain against a tendency to uniformly contract and thereby lower its electronic energy. $\Gamma = \pi\alpha/4$ eliminates this pathology. We note that the model Hamiltonian (1) has been used in several previous studies of defect energies in polyene chains.[20,22,31-33]

It is well known that an infinite chain described by Eq. (1) with one electron per site is unstable in the configuration $\{u_n = 0\}$ and will relax into a ground state described by

$$u_n = \pm (-1)^n u_0 . \quad (3)$$

This distortion introduces a gap at the Fermi level and the consequent gain in electronic energy drives the relaxation. As discussed in Ref. 27, we choose $t_0 = 3$ eV, $K = 68.6$ eV Å$^{-2}$, and $\alpha = 8$ eV/Å which yields a 12-eV $\pi$-electron bandwidth, a 1.4-eV Peierls gap, and an equilibrium distortion $u_0$ 0.0228 Å. These parameters provide a reasonable, though simplified, description of the optical threshold observed,[5,6,22] and bond alternation anticipated, in infinite *trans*-polyacetylene.

Several cautions concerning Hamiltonian of Eq. (1) are in order. First, while we will employ Eq. (1) to study the static properties of the polyene,

this Hamiltonian yields a description of the dynamics of the polyene which is deficient in three respects. (a) The zigzag planar nature of the polyene requires that inplane vibrations of the structure couple longitudinal and transverse motions of the atoms.[34] Such a possibility is excluded if one studies the temporal evolution of the scalar order parameter $\{u_n\}$. (b) The second term in Eq. (1) defines a potential well for the atom displacement which is perfectly harmonic. This is quite justifiable for static studies since we are interested in the value of the total elastic energy $U$ at some fixed configuration $\{u_n\}$. The fundamental quantities entering a lattice-dynamics study are, on the contrary, the second derivatives of $U$ in $\{u_n\}$. Thus, we may well expect that a harmonic form (1) while giving an acceptable description of the magnitude of $U\{u_n\}$, will poorly describe the curvature of this function. Indeed lattice-dynamics treatments of polyene chains[34-36] principally attribute the difference in single-bond and double-bond stretching frequencies to the anharmonic character of $U$, ignored in Eq. (1). (c) The H atoms are assumed to move adiabatically with the C sites. Again this is sensible for a static Hamiltonian but not for lattice dynamics where it is well established that H bending motions hybridize with C stretching motions in the polyene.[34-36]

The second principal difficulty with the Hamiltonian (1) is the approximate treatment of even the electronic contribution to the total energy. We take the electronic energy as a sum over the filled one-electron eigenvalues obtained from the first term in (1). Since the $\{t_{ij}\}$ implicitly include contributions from the electron-electron interaction this double counts the electron-electron contribution to the polyene energy. The empirical choice of the remaining terms in (1) corrects[38,39] for this error in the half-filled-band limit. However, for deviations from the half-filled band we ignore corrections to these effective lattice-energy terms due to changes in band filling. In view of this assumption and the approximate nature of the electronic term in (1) one expects the following results to be of only semiqualitative validity. These simplifying assumptions are ultimately useful as they allow us to compare the electronic spectra and stability of a large number of complicated structural configurations involving many atoms.

### B. Numerical methods

In the following calculations we will restrict our attention to long finite polyene chains. The chosen chain length is 256 atoms which is long enough to provide results which are representative of an infinite polyene chain and short enough to keep the evaluation of the electronic spectrum tractable. Direct diagonalization of the Hamiltonian is an inefficient procedure for eigenanalysis of a system of this size and we proceed with a continued-fraction expansion[40,41] for the diagonal Green's function for this system, which exploits the simple connectivity of the linear chain.

First we suppress the spin index and generalize the electronic Hamiltonian of (1) to include diagonal terms,

$$h=\sum \epsilon_n c_n^{\dagger} c_n+(t_{n,n+1}c_n^{\dagger}c_{n+1}+\text{H.c.}), \tag{4}$$

and introduce the resolvent operator $G(\epsilon)$,

$$G(\epsilon)=(\epsilon I-h)^{-1}. \tag{5}$$

The density of states, $n(\epsilon)$, is then

$$n(\epsilon)=\frac{-2}{\pi}\,\mathrm{Im}\,\mathrm{Tr}G(\epsilon) \tag{6}$$

so that evaluation of the diagonal terms in (5) allows a straightforward integration of the electronic energy of the system. Note that Eq. (5) defines a coupled set of linear equations for $G_{ij}(\epsilon)$:

$$\epsilon G_{ij}(\epsilon)=\delta_{ij}+\epsilon_i G_{ij}(\epsilon)+\sum_k t_{i,k}G_{kj}(\epsilon). \tag{7}$$

Iterative elimination of the off-diagonal terms in (7) shows that we may expand the diagonal Green's function at site $i$:

$$G_{i,i}(\epsilon)=\cfrac{1}{\epsilon-\epsilon_i-\cfrac{|t_{i,i+1}|^2}{\epsilon-\epsilon_{i+1}-\cfrac{|t_{i+1,i+2}|^2}{\vdots}}-\cfrac{|t_{i,i-1}|^2}{\epsilon-\epsilon_{i-1}-\cfrac{|t_{i-1,i-2}|^2}{\vdots}}}. \tag{8}$$

Thus the diagonal terms in (5) are obtained in a straightforward manner by a finite iterated sequence of divisions and additions. A power-series expansion of the right-hand side of (8) yields an infinite sequence of terms each of which may be interpreted as an independent real-space

excursion on the chain which starts and stops on site $i$. Though $G_{ii}(\epsilon)$ is singular at each eigenvalue of the structure, the problem is remedied by displacing the poles slightly from the real axis (i.e., $\epsilon \to \epsilon + i\delta$), which induces a Lorentzian broadening of the spectrum, $n(\epsilon)$. This Lorentzian broadening may make identification of true gaps in the spectrum difficult and more importantly makes the electronic contribution to the total energy logarithmically divergent.[35] Both of these difficulties are circumvented by deconvolution of the Lorentzian and reconvolution of a Gaussian line shape into the resultant spectrum. Though the density of states thus obtained never truly vanishes, we may in practice identify a gap as a region in which the density of states does not exceed a threshold value. We take as this value 0.005 states/eV atom which, though arbitrary, will be seen to accurately determine the presence of gaps in the following spectra.

Having determined the electronic spectrum, we calculate the free energy,[42]

$$F = \sum_n \mu - \ln(1 + e^{-\beta(\epsilon_n - \mu)})/\beta , \tag{9}$$

where $\beta = 1/k_B T$, the sum is taken over all the one-electron eigenstates and $\mu$ is determined by the requirement of particle conservation for $m$ electrons in the system at finite temperatures,

$$m = \sum_n \frac{1}{e^{\beta(\epsilon_n - \mu)} + 1} . \tag{10}$$

We present calculations for $k_B T = 10$ meV and note that even up to room temperature for most structures we will consider (9) is well approximated by a simple sum over the filled states. Finally, the evaluation of the remaining static terms in (1) is straightforward given a set of lattice coordinates $\{u_n\}$.

### C. Trial functions

In principle we should now proceed by seeking the set $\{u_n\}$ which minimize the free energy as calculated by the methods outlined in the previous section. In practice this requires the minimization of a complicated nonlinear function in a space of 256 dimensions, which is clearly an intractable task. We seek instead to minimize the energy in a restricted subspace of lattice displacements in which each solution is specified by one or two trial parameters. We define such a trial function as follows. We consider any lattice distortion to consist of a spatial modulation of the bond alternation $a$ given by Eq. (3), i.e.,

$$u_n = (-1)^n u_0(x) . \tag{11}$$

We know[19,20] that for band filling deviating from the half-filled band by a single carrier, the modulation (11) takes the form

$$u_0(x) = u_0 \tanh\left(\frac{x - x_0}{l}\right) , \tag{12}$$

while for deviation far from the half-filled band, $u_n$ should describe a periodic sinusoidal lattice distortion given by

$$u_0(x) = u_0 \sin(\delta q\, x) \tag{13}$$

with $\delta q = \pi \delta\nu / a$, $\delta\nu$ denoting the excess carrier concentration per site and $a$ denoting the nearest-neighbor separation on the chain. A continuous function which conveniently bridges these two limits is the elliptical sine,[43]

$$u(x) = u_0 \,\mathrm{sn}(\zeta x + \varphi; m) , \tag{14}$$

with a period $\zeta = 4K(m)$ where $K$ is the complete elliptical integral of the first kind. The character of the function is defined by the modulus $m$ ($0 \leq m \leq 1$). For $m = 1$ $u(x)$ describes a periodic array of solitons (i.e., tanh-like solutions) and as $m$ decreases from 1 the sn rapidly becomes sinusoidal in character. Thus the magnitude of $m$ becomes significant only when $m$ approaches 1. In this limit we can adopt the continuum results of Rice and Timonen[44] which fixes the modulus of $m$ to the excess carrier density $\delta\nu$:

$$4K(m)[2(1+m)]^{1/2} = 2a/\delta\nu l_0 , \tag{15}$$

where $4l_0$ is a full soliton width which is roughly $10a$. Equation (15) has no solution for $\delta\nu$ past a critical concentration $\delta\nu^*$ given by

$$\delta\nu^* = a/2\pi l_0 , \tag{16}$$

in which case it it clear that we require $m = 0$ (i.e., a sinusoidal modulation) in Eq. (14). Thus the prescription for the definition of the modulus of $\mathrm{sn}(\zeta x; m)$ in the trial function is to take the solution to (10) for $\delta\nu < \delta\nu^*$ and $m = 0$ for $\delta\nu > \delta\nu^*$. The wave vector $\zeta$ of the function is further specified by requiring the elliptical sine to exhaust a half period in the interval $a/\delta\nu$,

$$\zeta(m) = \frac{\delta\nu}{a}[2K(m)] . \tag{17}$$

This completes the specification of the trial solution for a uniformly incommensurate structure, which we will discuss further in Sec. IV. Only one free parameter specifies the trial solution, the amplitude $u_0$. This is variationally determined by minimizing the free energy in the space described by the trial solution (14).

We will also be concerned with the effects of disorder on a modulation of the bond alternation of the form (11). This disorder with which we

are concerned is that due to the impurity sites. We model this alternatively by considering the coupling of $\pi$ electrons on the polyene to impurity sites via a screened Coulomb interaction or by considering the local modification of $\pi$-electron basis orbitals adjacent to the impurity. In either case, we anticipate that the principal effect of disorder is to spatially distort the modulation $u_0(x)$ of Eq. (14). For sufficiently strong disorder one expects excess charge on the polyene to congregate near the impurity sites, hence in a solution of the form (14) we expect the modulus of the trial function to be spatially modified as well. We formally include this degree of freedom as follows. Note that the solution (14) describes a trial function with a set of equidistant nodes $\{x_n\}$ where

$$x_{n+1} - x_n = a/\delta\nu \,. \tag{18}$$

For a charge density wave which is severely pinned in the presence of a strong impurity potential the nodes will be locked on to the impurity sites $\{y_n\}$.[45] For intermediate disorder we anticipate a continuous evolution of the lattice distortion between these two limits. Let us then define a modulation of the bond alternation of the form (11) in which $u(x)$ has nodes at

$$p_n = \beta x_n + (1-\beta) y_n \,. \tag{19}$$

$\beta$ is a continuous variable in the range $0 \leq \beta \leq 1$, which describes the continuous evolution of the system between these two limits. Note that in the free length of chain between any two adjacent nodes we define a local excess density $\delta\nu(x) = 1/(p_{n+1} - p_n)$. This is in turn used to define the local modulus of the trial function via relation (15). As previously, the local "wave vector" $\zeta$ is given by Eq. (17) which requires that we exactly fit a half period of the elliptical sine in the interval $p_{n+1} - p_n$. Sample trial functions $u(x)$ for a 256-atom chain doped with ten impurities randomly situated adjacent to the chain are given in Fig. 1 for various value of $\beta$. As $\beta$ decreases from unity the function $u_0(x)$ is increasingly strongly phase distorted and finally becomes exactly commensurate with the *impurity* lattice at $\beta = 0$. Note that our choice of the form of the trial function allows the system to recover sections of uniform bond alternation in regions where the distance between adjacent impurities becomes large. In our calculations of chains disordered by an impurity potential both the amplitude $u_0$ and the pinning parameter $\beta$ are variationally determined by minimizing the free energy.

There are two refinements of the trial solution of this kind which are worth noting. First, our construction (19) describes a uniform shifting of the nodes in $u(x)$. Physically one expects larger shifts of this kind in regions where $m$ approaches 1; i.e., in regions where the zero crossing has the character of a domain wall. Such a tendency could be incorporated in a straightforward manner in a trial function of this kind, although we have not explored this possibility. Second, one may anticipate a local modulation of the amplitude of the elleptical sine which would also be determined by the local density. That is, at very high densities one eventually expects some suppression of the magnitude of the bond alternation in sections of the chain. Though this mechanism has previously been offered in explanation of the insulator to metal transition in $(CH)_x$,[44] we here note that bond alternation is experimentally observed in very short polyenes[37] and in the next section we will discuss calculations which show a reduction of bond alternation by only a factor of 3 even when the nodes in $u(x)$ are as close as seven lattice spacings. Thus, we expect only slight improvement of our trial function by incorporating such an effect.

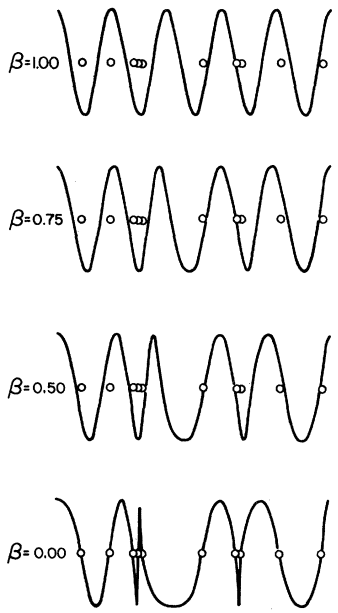


FIG. 1. Trial functions for the spatial modulation of the amplitude of bond alternation $u_0$ for various values of $\beta$ in a 256-atom chain. The circles mark the chain positions adjacent to the ten impurity sites.

## III. IDEALLY INCOMMENSURATE STRUCTURE

In this section we consider the relaxation of a finite polyene chain which is charged by the addition or deletion of a specified number of

electrons. We ignore the presence of the impurity atoms and thus consider the trial solutions described in Sec. II C with $\beta = 1$ and $u_0$ taken as a variational parameter. We refer to such structures as ideally incommensurate. This investigation amounts to an assessment of the strength of the Peierls instability in $(CH)_x$ as we proceed away from the half-filled band. The one-dimensional system must distort for arbitrary band filling opening a gap separating the highest filled and lowest empty one-electron levels; here we consider the magnitude of the distortion and the size of the gap one should expect in such a situation.

In Fig. 2 we show densities of states obtained in the ground-state configuration for a variety of polyenes doped to the concentrations shown in the insets. There is a striking regularity in these spectra. At low concentrations we obtain a narrow band which is associated with a lattice of isolated solitons, i.e., kinks in the amplitude of the bond alternation as given by Eq. (14) with $m \approx 1$. The Fermi energy for acceptor doping is given by the large vertical bar. In the midgap band the dopant induced holes are paired with an equal number of "holes" from previously umperturbed conduction band. The ground state is thus always diamagnetic. The threshold for single particle excitations is the energy from the valence-band maximum to this midgap defect band, i.e., half the original bandgap or 0.7 eV.

As one proceeds to higher dopant concentrations we observe that this midgap "band" simply grows, always accommodating the excess dopant induced charge on the polyene with an equal number of empty states from the original conduction band. As required by Peierls theorem the Fermi energy always falls in a gap, and noting that the electronic spectrum in Eq. (1) must exhibit symmetry about the level $\epsilon = 0$, a companion gap is always obtained in the manifold of empty levels above $\epsilon_F$. The midgap band thus defined represents a "condensate band," i.e., a frequency regime in which added charge and intrinsic charge on the polyene condense and separate from the valence and conduction continua. Evidently, the system elects to undergo a distortion with maximum economy as the one-dimensional spectrum is completely unaffected except for the emergence of this gap at the Fermi level (and its companion gap in the conduction band).

As one proceeds far from the half-filled-band limit, the resulting spectra resemble the spectra one would anticipate from the usual treatment of the incommensurate charge density wave in a one dimensional system.[13,14] That is, states at $k_F$ and $-k_F$ are strongly mixed by perturbing

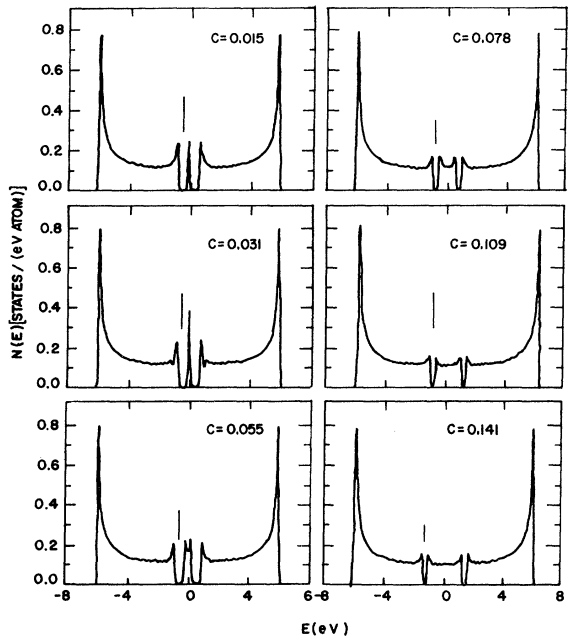


FIG. 2. Densities of states for $\pi$ electrons in $(CH)_x$ in uniformly incommensurate structures for the doping concentrations listed in insets. The vertical line marks the Fermi level in each configuration.

terms in the Hamiltonian which result from a lattice distortion peaked at wave vector $q = 2k_F$, and a gap is opened in the spectrum of one-electron eigenstates. Clearly this treatment breaks down in the limit that $2k_F$ approaches $\pi/a$. Close to the half-filled bands there is strong interference between the mixing of states at $k_F$ and $-k_F$ and those at $(\pi/a - k_F)$ and $(-\pi/a + k_F)$, the latter coupling to the phonon distortion at $2k_F$ through an umklapp process in the field of the underlying lattice potential. In this regime the lattice distortion is poorly described by a single Fourier component and the modulus of the trial function (14) closely approaches unity. The tanh-like solution to (14) is then readily understood as the self-consistent response of the lattice in the presence of a strong modulation of the responding charge density at the higher harmonics of a single Fourier component of the lattice deformation potential.[46] The critical concentration at which such mixing becomes significant is defined by the size of the dimensionless expansion parameter $|\Delta/\hbar w_F \delta q|$ where $2\Delta$ is the Peierls gap for the half-filled band, $v_F$ is the Fermi velocity in the metallic (undistorted) state and $\delta q = \pi \delta \nu / a$, $\delta \nu$ denoting the excess charge per atom on the chain. When the parameter is of order unity the electron density will be strongly perturbed at the odd harmonics of $\delta q$, which in turn induces

a lattice distortion at these higher wave vectors.[46] For the present model for $(CH)_x$ this occurs for $\delta n$ below a critical concentration $\delta\nu_c$ where $\delta\nu_c \sim 0.04$.

In Fig. 3 we examine the behavior of the modulated $\pi$-electron charge density as $\delta\nu$ passes through this threshold. All the plots exhibit a rapid oscillation with wavelength $2a$; however, we are interested in the long-wavelength envelope which modulates this oscillation. For $c=0.015$, well below the critical concentration, the excess charge is well localized on the nodes which occur in $u(x)$. As $c$ progresses past the threshold the charge is seen to begin to delocalize on the polyene. Finally for $c=0.109$, well above the threshold concentration, the envelope has a simple sinusoidal form, and an average over the rapid oscillations shows that charge is uniformly distributed on the chain. Clearly the effect of the higher harmonics below $\delta\nu_c$ is to localize charge to isolated defects on the chain, thus allowing recovery of regions of uniform commensurate bond alternation. Note that for $\delta\nu < \delta\nu_c$ the kinks thus obtained interact only weakly and thus the $\pi$-electron spectrum of the system would be insensitive to translations of these defects as might occur in the pinning potential of an ionized impurity, for instance. For $\delta\nu \gg \delta\nu_c$ the spectra will be strongly perturbed by such periodicity breaking phase distortions. This observation provides the basis for our discussion of the effects of disorder due to impurities in Sec. V.

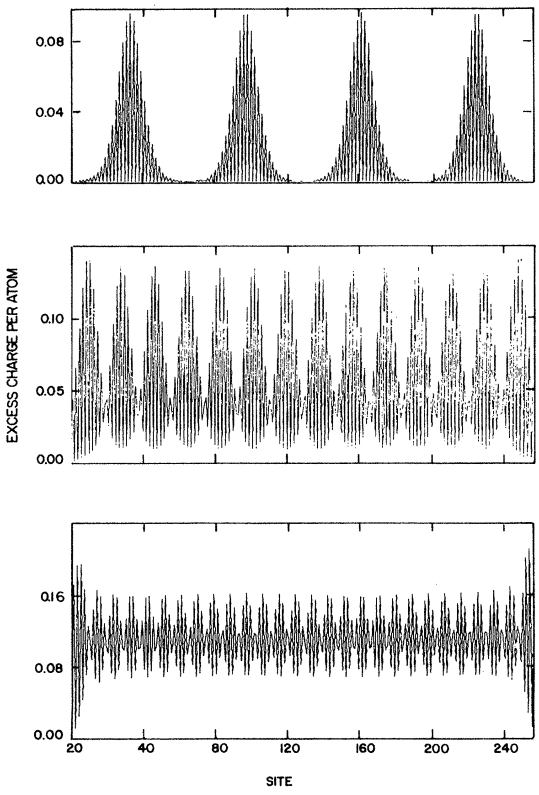


FIG. 3. Distribution of the *excess* charge density in a $(CH)_x$ chain in the uniformly incommensurate structures obtained at the doping concentrations of 1.6, 5.5, and 10.9 at.%.

In Fig. 4 we examine the dependence of the order parameter $u_0$ and the Peierls gap $E_g$ on the excess $\pi$-electron density. Again the critical concentration $\delta\nu_c$ provides a useful benchmark for interpreting these results. For $c < \delta\nu_c$ the localization of the excess charge to kinks in the bond alternation on the polymer leaves large regions which are unaffected by the excess carriers. Hence the order parameter $u_0$ is largely determined by these unperturbed regions and recovers to its half-filled band value. For $c > \delta\nu_c$ the full chain is uniformly distorted and the order parameter decreases from this half-filled-band value. We obtain a minimum value $u_0 = 0.01$ Å just below $c \sim 0.10$ and thereafter $u_0$ increases again as $c$ approaches the next concentration which will be highly commensurate with the underlying lattice. At such highly commensurate densities the $\pi$-electron gas will be especially susceptible to static modulations of the charge density and hence will support larger values of $u_0$.

After addition of the first carrier to the polyene, $E_g$ drops to 0.7 eV, half the value for the neutral chain, and smoothly tracks the order parameter $u_0$ thereafter. Note that we do not obtain a precipitous drop in the gap as a function of increasing dopant concentration. Over the concentration range in which the insulator-metal transition is experimentally observed, $E_g$ always exceeds 0.5 eV and even for dopant concentrations up to 14 at.% the gap is of order 0.25 eV. Noting that the parameters in our model provide the smallest reasonable gap for the neutral $(CH)_x$ chain, we

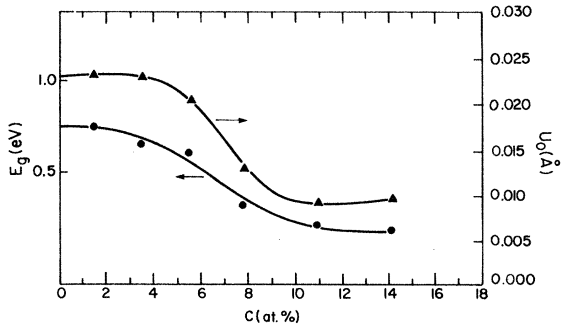


FIG. 4. Peierls gap $E_g$ and order parameter $u_0$ as functions of dopant concentration for the ideal incommensurate structures.

expect that these energies are lower bounds for the Peierls gaps expected at these dopant levels.

Thus the Peierls instability in $(CH)_x$ is a very formidable obstacle to metallic behavior even at very high dopant levels. (We note in passing that this simple model is not inconsistent, in principle, with the specific observation of enhanced conductivities in samples below 5 at.% impurity concentration, as these incommensurate structures conduct via a sliding mode mechanism.[13] However, the Peierls ground state is incompatible with the preponderence of experimental data[23,47-49] which indicate the existence of a finite density of states at the Fermi level in the "metallic" state.) Having noted that the ideal doped system exhibits a rather strong tendency to seek an insulating ground state, we consider, in the next section, the nonideal characteristics of the real system which are particularly likely to suppress this tendency.

## IV. DISORDER AND THREE DIMENSIONALITY

The treatment of Sec. III focused on the response of the polyene to excess charge in the $\pi$ manifold while ignoring the effect of the ionized dopant sites which are the source of this charge. In the following we consider the ionized dopants to reside at random sites adjacent to the chains to which they have donated charge. In such a configuration we conceive of two important possible perturbations introduced by the dopant.

First, the dopant may have chemically attacked the polyene.[50] That is, one may consider the charge transfer to result from the formation of a bond between the dopant and a polyene $\pi$ orbital which has a large ionic character. We may describe such a bond a simple $2\times 2$ linear combination of atomic orbitals model. We define two basis orbitals $\varphi_C$ and $\varphi_D$ which denote orthogonal functions localized on the carbon $p$ orbital and the singly occupied dopant level, respectively. The diagonal Hamiltonian matrix elements in these states are $\epsilon_C$ and $\epsilon_D$, respectively, whose difference is expected to be large. For definiteness we consider the case of acceptor doping where $\epsilon_D \ll \epsilon_C$. In the presence of a mixing term $V$ the new eigenstates at the site are

$$\varphi_+ = a\left(\varphi_C - \frac{V}{\epsilon_D - \epsilon_+}\varphi_D\right),$$
$$\varphi_- = a\left(\frac{V}{\epsilon_C - \epsilon_-}\varphi_C - \varphi_D\right), \tag{20}$$

with eigenvalues

$$\epsilon_\pm = \tfrac{1}{2}\{\epsilon_C + \epsilon_D \pm [(\epsilon_C - \epsilon_D)^2 + 4V^2]^{1/2}\}.$$

The lower filled state describes charge transfer to a bonding level primarily localized on the dopant, the upper antibonding level is primarily localized on the polyene. Mixing with other states on the polyene occurs primarily through the upper antibonding level; hence we ignore the bonding state and redefine an effective $\pi$-electron Hamiltonian in which the diagonal matrix elements on such bonded sites are displaced by $V = \epsilon_- - \epsilon_C$. This introduces a random diagonal potential in the Hamiltonian of Eq. (1) and depending on the strength $V$ we expect distortions of the lattice configuration discussed in Sec. III to result. We refer to this model as the covalent-bond model.

A second important possible consequence of the proximity of an ionized dopant molecule, which differs in spirit from the covalent bond model, but induces a similar effect, is simply a pinning potential on the chain due to the screened Coulomb interaction with $\pi$ electrons on the polyene. This represents a long-range analog of the effect described by the covalent-bond model. One proceeds in principle to screen self-consistently the $1/r$ potentials induced on the chain by the dopants. In the following we approximate this screened potential by a static screening of the ion potentials, defining a diagonal potential for the $n$th $\pi$ orbital on the chain:

$$\epsilon_n = \sum_i v\left[1+\left(\frac{x_n - x_i}{d}\right)^2\right]^{1/2}, \tag{21}$$

with $v = 0.6$ eV, $d = 2$ Å, $x_n$ denotes the location of the $n$th $\pi$ orbital on the chain and the sum is over sites adjacent to impurity positions. This effect also induces a random diagonal potential on the chain which is similarly expected to disorder the response of the underlying lattice. We refer to this model as the Coulomb-coupling model. In both calculations on the covalent bond model and the Coulomb-coupling model the impurity sites are selected at random until the chain is doped to the desired density.

Finally we recall that the real system is only quasi-one-dimensional and we must ultimately be concerned with the presence of a three-dimensional network of weakly interacting chains. To expolit the efficiency of the numerical techniques described in Sec. II B we model this 3D network by a finite Cayley tree[40] with anisotropic interactions. The Cayley tree is in fact an infinite-dimensional network, but for the present application it is best described as a mathematical lattice which contains no closed rings, so that any two points in the lattice are linked by only one path of bonds. In such a lattice one may straightforwardly generalize the continued-fraction expansion (8) to obtain the diagonal Green's function at any site in the network. In the pre-

sent model, at each site in the lattice we couple strongly to two nearest-neighbor sites (representing nearest neighbors on the same chain) and weakly to $z$ nearest neighbors (which represent neighbors on adjacent chains). We take $z=6$ (representing close packing in the two dimensions transverse to the chain axis[51]) and adjust the interchain overlap integral to provide an interchain bandwidth of 0.2 to 0.3 eV near the Peierls edges.[7] The strong nearest-neighbor interaction integrals are parametrized in the form of Eq. (3). The treelike network, thus constructed, ignores ring-like interaction paths which are introduced into the system by interchain coupling. However, we note that the only effect of the increased dimensionality is to provide a slight shift of the band edges of the 1D spectra and thus we expect only a slight dependence of this shift on the *details* of the interchain Hamiltonian.

In our 3D calculations which include a random impurity potential, constructed as described earlier in this section, each one-dimensional limb of the multidimensional network is doped to an identical density, and the impurity distribution on each limb is given by a cyclic permutation of the impurity distribution on the other limbs. This prevents charge transfer between such 1D limbs and allows us to consider a trial function of the form (14) with a common pinning parameter $\beta$ for all the chains. The diagonal Green's function, written in the form (8), is then summed over the centermost 1D limb in this multidimensional network and the free energy is minimized with respect to the variational parameters $u_0$ and $\beta$.

We observe lastly that modelling the three-dimensional network by a Cayley tree in this manner provides an attractive alternative to inclusion of a lifetime broadening of the one-dimensional spectra due to phenomenological 1D mean free path (or correlation length) in the presence of a 3D potential.[52,53] In the former approach band edges are shifted but remain well defined (as one expects in the true system) whereas in the latter approach the long tails induced by the Lorentzian make identification of true band edges difficult.

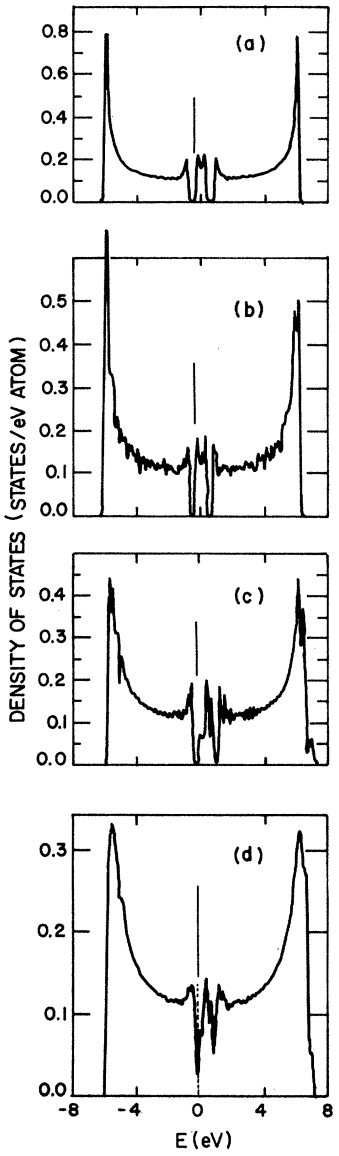


FIG. 5. Densities of states for $\pi$ electrons in $(CH)_x$ with 5.5 at.% acceptor doping: (a) ideal incommensurate structure, (b) impurity potential treated in the covalent-bond model (c) impurity potential treated in the Coulomb-coupling model, and (d) impurity potential treated in the Coulomb-coupling model and 3D interactions included. The vertical bar gives the Fermi energy in each configuration.

## V. DISORDERING OF THE INCOMMENSURATE CHARGE DENSITY WAVE

In Fig. 5 we examine the effects of the disordering influences outlined in the preceding section on the electronic spectra calculated at a 5.5 at. % concentration of acceptors. The top panel (a) is for reference and shows the spectrum obtained for the ideally incommensurate structure which we calculate ignoring the impurity potential. In panel (b) we show results obtained by treating the impurity potential in the chemical bond model with $v=1$ eV. At this interaction strength the equilibrium solution occurs at $\beta=0$; i.e., the charge density wave is optimally pinned to the impurity sites. The diagonal random potential in-

troduced in this model has the effect of introducing penetrable barriers on the chain which thus tends to break our very long chain into rather short finite segments. This in turn introduces the scatter in the eigenvalue spectrum which is seen in Fig. 5(b). The midgap condensate band is still prominent, though it is broadened slightly by the random potential. This effect and the broadening of the valence band edge reduce the gap from its uniformly incommensurate value of ~0.6 eV to just below 0.4 eV.

Generally similar results are obtained for the Coulomb-coupling model shown in Fig. 5(c). Again the equilibrium solution has the charge density wave optimally pinned with $\beta = 0$. The effects of the random potential on the condensate are more pronounced in this model; however, this feature is still prominently separated from the valence and conduction continua. The gap between the highest filled and lowest empty levels is further suppressed to ~0.3 eV in this model.

Finally Fig. 5(d) shows the results treating the impurity potential in the Coulomb-coupling model and including 3D interactions with other chains in the solid. Here again the lattice distortion is commensurate with the impurity potential with $\beta = 0$. Unlike the results in 5(b) and 5(c) the gap between the valence band and condensate has *closed*, with the Fermi energy located at the level given by the dashed line. Nonetheless spectral features due to the condensate band are still quite evident in this spectrum. In fact the amplitude of the order parameter $u_0$, recovers to 75% of its half-filled band value at this concentration. In this structure the order parameter is thus stabilized by a pseudogap rather than a true gap in the density of states.

There are two important points which are illustrated by this survey at a 5.5 at. % impurity concentration. First, we see that reasonable estimates of the random potential due to impurities indicate that the incommensurate charge-density-wave solutions discussed in Sec. III are likely to be strongly pinned at this concentration. While one expects the CDW to become more resilient at higher concentrations, we note that for all concentrations we have studied in which the order parameter $u_0$ is stabilized at a non-negligible value, an equilibrium $\beta \leq 0.25$ is obtained. Thus for all concentrations at which we may sensibly speak of a charge density wave in the system, the lattice distortion is expected to be strongly pinned by impurity sites. Second, we note that the concentration treated in this example is very close to the observed insulator-metal transition density in polyacetylene. While we will deal with this transition in more quantitative detail in the next section we presently remark on the relative contributions of the strictly one-dimensional disorder and three-dimensional coupling to the suppression of insulating behavior at $c = 0.055$. From the trends displayed in Fig. 5 we conclude that 1D disorder and 3D coupling are of roughly equal importance in suppressing the 0.6-eV incommensurate gap and thus producing a metallic state by a 5.5 at% impurity concentration. A reduction of the gap by several tenths of a volt can be reasonably attributed to either effect separately, so that the combined effect is likely to close

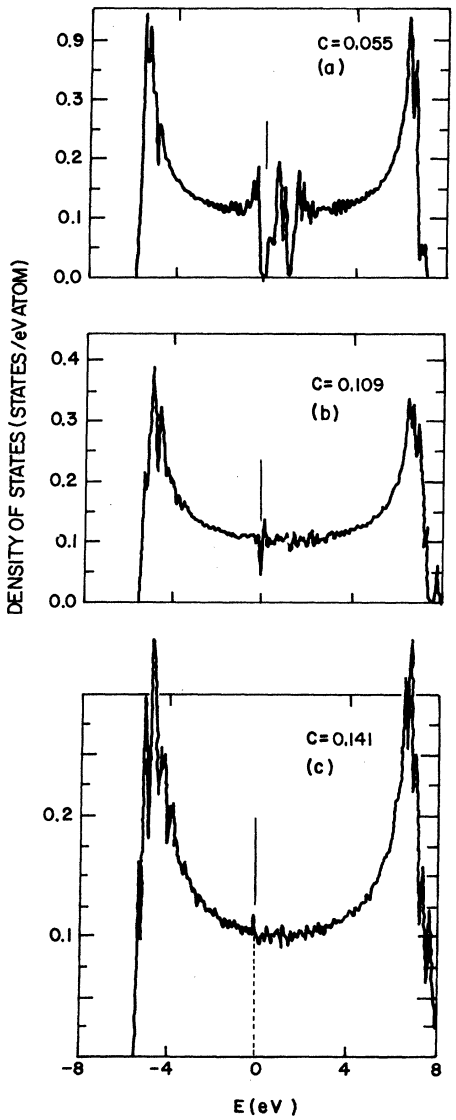


FIG. 6. Densities of states for $\pi$ electrons in $(CH)_x$, doped with acceptors to the concentrations shown in the insets, including an impurity potential treated in the Coulomb-coupling model. The Fermi energy in each configuration is given by the vertical bar.

the ideal incommensurate gap at this concentration. Note that in spite of the rather severe spectral smearing, the Peierls instability remains very strong in this system as evidenced by the deep pseudogap and large amplitude of the order parameter which persist in Fig. 5(d).

## VI. THE INSULATOR-METAL TRANSITION

In this section we examine the behavior of the density of states and order parameter obtained in both one-dimensional and three-dimensional disordered models as we proceed through the insulator-metal transition. We consider first the one-dimensional models. The results for the covalent-bond model and the Coulomb-coupling model are similar; in the following we restrict our attention to results employing the Coulomb-coupling model. In Fig. 6 we show spectra obtained for equilibrium configurations at three concentrations as we proceed through an insulator-metal transition. The top panel is for $c=0.055$ [identical to Fig. 5(c)] in which a gap of 0.3 eV is obtained as shown and as described earlier. At $c=0.109$, shown in the second panel, we have just crossed the 1D transition density. The system is characterized by a finite density of states at the Fermi energy but a pseudogap or deep depression in the density of states persits. Finally at very high concentrations, e.g., $c=0.141$ in panel (c), the amplitude of the order parameter is strongly suppressed as well and the pseudogap disappears from the density of states.

The evolution of the metallic character and order parameter of this system through this transition are examined in Fig. 7. A gap persists in the spectrum up to a concentration near $c=0.08$. Above $c=0.10$ the Fermi level state density increases rapidly, finally saturating at a one-dimensional midband value at $c=0.141$. The amplitude of the order parameter $u_0$ remains close to its half-filled band value up to $c=0.05$. Thereafter, $u_0$ is gradually suppressed by the increased disorder in the system. Note that near the metallic threshold ($c\approx 0.10$). $u_0$ is quite sizable and is suppressed only slightly from its ideal incommensurate value (see Fig. 4). Thus bond alternation persists into the metallic state which occurs just above this critical concentration. For still higher concentrations bond alternation is severely depressed in the presence of increased disorder. In these calculations, $u_0$ does not vanish but is negligibly small for $c \geq 0.14$. The concentration range over which there is no gap, but bond alternation is stabilized by a pseudogap, is quite small extending for $\delta c=0.04$ above a threshold near $c=0.08$. (This regime in which a gapless Peierls distortion is obtained appears quite similar to the gapless stabilization of a condensate known in dirty superconductors.[54])

The picture which emerges from the three-dimensional models is qualitatively similar. Electronic spectra for three representative equilibrium configurations near the insulator-metal transition are given in Fig. 8. For $c=0.031$, just above the transition, a very deep pseudogap is obtained, at the center of which is positioned the Fermi level. A smeared remnant of the condensate band is evident in this spectrum above the Fermi level. As the dopant concentration increases we obtain a gradual filling in of this pseudogap which is seen to track the Fermi energy through the $p$ bands. For $c=0.078$ the pseudogap is evident as a slight depression in the density of states; by $c=0.109$ it is entirely filled in.

The behavior of the Fermi level state density and the order parameter as a function of dopant concentration in the 3D models are investigated in Fig. 9. A gap occurs at very low concentration, finally being closed at an impurity concentration near 2 at. %. Thereafter the density of state at the Fermi energy increases smoothly, eventually saturating at a concentration near 10 at. %. As expected, the order parameter remains close to its half-filled band value, beginning a smooth descent near $c=0.03$, and finally becoming severely depressed above $c=0.10$. As in the one-dimensional calculations the metallic state just above the transition is characterized by a nonzero-order parameter. The bond alternation found in this regime is again stabilized by a pseudogap in the electronic spectrum, and indication of the underlying strength of the Peierls distortion in this system. The severe depression of $u_0$ below 0.005 Å near $c=0.10$ may be interpreted as a further structural transformation to a

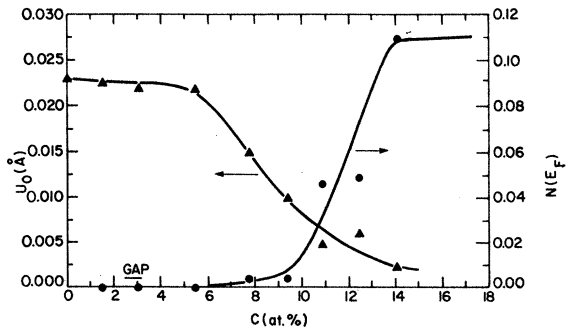


FIG. 7. Fermi level density of states, $N(\epsilon)$, and order parameter $u_0$ for the one-dimensional disordered models for doped $(CH)_x$ as a function of dopant concentration $c$.

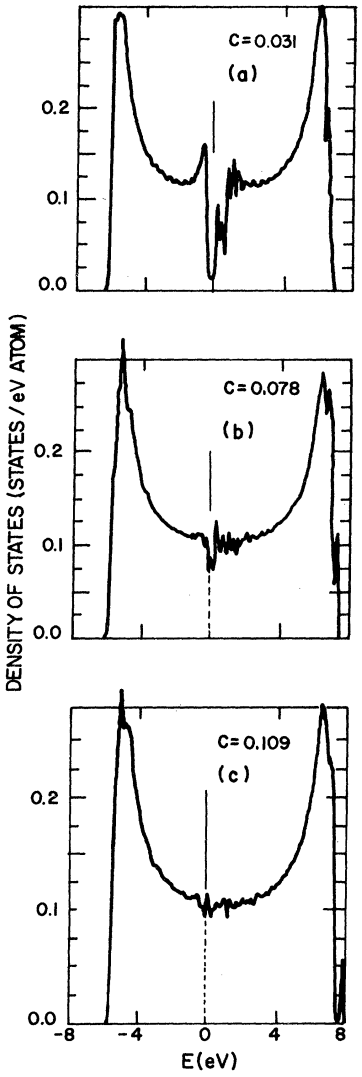


FIG. 8. Densities of states for $\pi$ electrons in a multidimensional model for $(CH)_x$, doped with acceptors to the concentrations shown in the insets, including disorder in the Coulomb-coupling model. The Fermi energy in each configuration is given by the vertical bar.

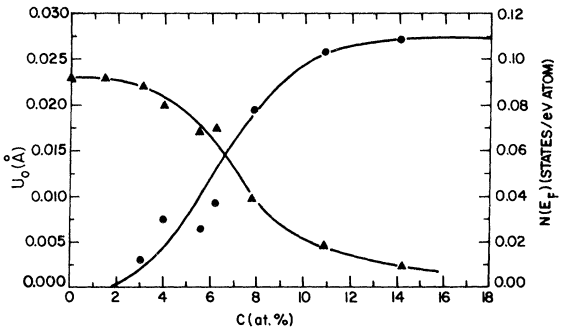


FIG. 9. Fermi level density of states, $N(\epsilon)$, and order parameter $u_0$ for the multidimensional disordered models for doped $(CH)_x$ as a function of dopant concentration $c$.

(nearly) uniform bond length metallic state.

The three-dimensional disordered models thus studied differ from the one-dimensional disordered models in two important ways. First the one-dimensional transition density (~10%) is suppressed to near 3% by three-dimensional coupling, (nearly where it is observed experimentally). Second, the concentration range over which the order parameter persists into the metallic state is significantly larger in three dimensions than in one dimension. Evidently the important consequences of the three-dimensionality of this system are thus a suppression of the transition density and a smearing of this transition as a function of concentration.

From these calculations we conclude that the insulator-metal transition in polyacetylene involves the following elements. First, in the concentration range over which the transition is experimentally observed, simply the addition of charge to the polyene is responsible for a reduction of the gap by about a factor of 3. This reduction is an intrinsic Peierls effect and occurs as the polyene spatially modulates the amplitude of its bond alternation with a wavelength incommensurate with the underlying lattice. Second, the presence of ionized dopants near the chain introduces a random diagonal potential in the Hamiltonian describing the $\pi$ electrons on the polyene. In response to this random diagonal perturbation the ideal incommensurate wave is severely distorted on the polyene, strongly preferring a structure which is commensurate with the *impurity* potential. This introduces strong off-diagonal disorder on the polyene as well. The combined effects of these two disordering influences are to broaden band edges, and these one-dimensional effects will themselves lead to an insulator-metal transition near a 10 at. % dopant concentration. Third, a slight broadening due to interchain interactions contributes to this closing of the gap and is reasonably expected to suppress this transition density to ~3% where it is seen experimentally. Fourth, in either a one-dimensional or three-dimensional theory bond alternation persists into the metallic state. For very high concentrations past this initial transition we expect a further structural transformation in which bond alternation is itself suppressed to negligible values. Fifth, the electronic states which occur at the Fermi energy in the strongly

disordered structures just above the insulator-metal transition are expected to be localized.

## VII. FLUCTUATIONS AND EXPERIMENTAL IMPLICATIONS

In the preceding we have focused on the structural response of a finite polyene ($N=256$ atoms) to the presence of a random distribution of a specified number of dopant atoms. We note however that the electronic spectrum of a homogeneously randomly doped macroscopic sample is *not* correctly given by these results on a single finite sample doped to an equivalent density. (By homogeneous doping, we mean that the mean density averaged over a macroscopic volume does not depend on the region of the sample over which the average is taken.) In the true system, doped to a concentration $c$, we expect that in an $N$-atom sample selected at random there is always a nonzero probability $P(n;N)$ that $n$ impurity sites will be found where

$$P(n;N)=\frac{N!}{n!(N-n)!}c^n(1-c)^{N-n}. \tag{22}$$

Thus when considering any macroscopic experimentally determined parameter $y$ in this system we should adopt a statistical point of view in which we weight the result of a measurement at any density $c'$ by the probability of its occurrence at an average density $c$. That is,

$$\langle y\rangle_c=\sum_{n=0}^{N}P(n;N)y(n). \tag{23}$$

Clearly we require $N$ to be large enough that we can sensibly speak of the measurement $y$ in this sample population. For the transition under consideration in polyacetylene $N$ is evidently manageably small. For $N=256$ atoms we have identified, to a resolution $k_BT$ at room temperature, a continuum of electronic states at the Fermi level, and the concomitant metallic response of the population. This is so despite the fact that such a test population may contain only 10–20 impurity sites at the semiconductor-metal transition. Thus near the transition dopant density we certainly expect fluctuations in the local dopant density to significantly affect the result of any macroscopic measurement on the sample. Physically this occurs because the metallic structure involves a response of all the $\pi$ electrons in the polyene, but is locally driven by the presence of a relatively small number of added carriers. This behavior is in marked contrast to that of an impurity-band insulator-metal transition in which $N$ is properly chosen to include a large number of *dopant* sites, $n$; hence fluctuations on the order $1/\sqrt{n}$ are strongly suppressed.

Adopting this point of view we have calculated an ensemble average of the Fermi level density of states for both the one-dimensional and three-dimensional models we have discussed in Sec. VI as a function of average impurity concentration $c$. The results are given in Fig. 10. In both one and three dimensions the density of states at the Fermi level exhibits a smooth onset, gradually increasing and saturating at 0.11 states/eV atom. The presence of a finite density of states at the Fermi level, even at negligibly small impurity concentrations is due to the statistical chance of finding a locally dense quasimetallic region at any macroscopic concentration $c$. Note that in this theory, the occurrence of such quasimetallic regions is a purely statistical event, and does not require a correlated aggregation of impurities forming macroscopic metallic islands. (Such inhomogeneous aggregation may occur in a real system[49,55,56]; we emphasize, however, that such correlated "island" growth is not required to explain quasimetallic behavior at very low concentrations.) The probability of the occurrence of such regions below $c=0.03$ in our one-dimensional theory is indeed infinitesimally small (the local concentration must exceed 0.08 for significant metallic behavior). However in three dimensions the intrinsic "transition" dopant density is sufficiently small that one expects a measurable quasimetallic volume even for $c\approx 0.01$. The saturation of the density of states at 0.11 states/eV atom in these calculations marks the onset of the high concentration regime in which even bond alternation is strongly suppressed in the presence of strong disorder due to impurities in the sample.

Finally we should comment on the relevance of these theoretical observations to several experi-

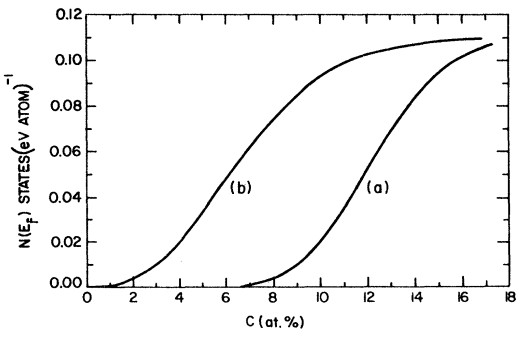


FIG. 10. Ensemble averaged Fermi level densities of states, $N(\epsilon)$, for (a) one-dimensional and (b) three-dimensional models as a function of macroscopic dopant concentration, $c$.

mental probes of the metallic character of doped samples. From the arguments just given we would expect a direct probe of the Fermi level state density, like the Pauli susceptibility, to show a smooth turn on near 2–3 at. % dopant density, increasing smoothly and eventually saturating at a "metallic" value (~0.11 states/eV atom) near $c = 0.09$–$0.10$. Such behavior has been reported by Epstein *et al.*[23] for $I_3$-doped $(CH)_x$ and similar results have been obtained with other dopants as well. $I_3$, which is known to aggregate, may present a particularly pathological dopant to interpret within a statistical theory. The reported presence of a small nonzero Pauli susceptibility for $c \leq 0.01$ (Ref. 49) is understandable in terms of the inevitable local dopant density fluctuations described above.

Next we consider the ultimate figure of merit for assessing the metallicity of these samples, namely their conductivities. We expect that due to the reduced dimensionality and complicated (and poorly understood) morphology of these systems, that a reliable description of the dc conductivity is an elusive goal. Nevertheless, we proceed as follows. Note that the states we have found at the Fermi energy are expected to be localized due to disorder induced by the impurities; thus the intrinsic transport mechanism is expected to be a hopping process. Let us assume that this hopping at $\epsilon_F$ is described by a simple variable range hopping model.[30] We can then use the ensemble averaged Fermi level state density to estimate the mean hopping distance and hence the concentration dependence of the conductivity at a fixed temperature. It is unclear whether a one-dimensional or three-dimensional hopping description is to be preferred in this context; results for both theories at $T = 300$ K are given as a function of dopant concentration in Fig. 11. In these calculations we assume a localization length along the polymer axis of 50 bond lengths; the results are weakly sensitive to this choice and we expect a value between 10 and 100 lattice spacings to be realistic. The important result is that the conductivity shows a sharp increase at concentrations below 2 at. % and rolls over to a saturation value near 3–5 at. % impurity concentration. The conductivity below 2 at. % is almost certainly due to hopping between the quasimetallic regions we have attributed to impurity density fluctuations. At densities above 5 at. % we obtain hopping in a dense spectrum of localized levels. The shoulder on these curves may be estimated to occur at the density at which the mean hopping distance is on the order of the localization length at the Fermi energy. Note that in this three-dimensional theory this always occurs near or below $c = 0.05$ (while

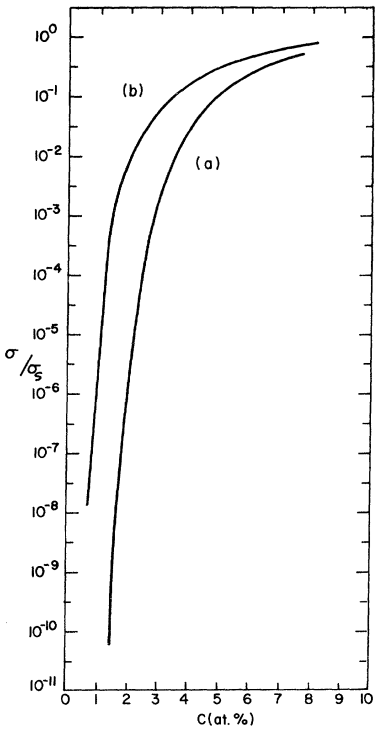


FIG. 11. Conductivity at 300 K estimated from a variable range hopping model based on our 3D electronic structure for doped $(CH)_x$ : (a) assumes one-dimensional variable range hopping and (b) assumes three-dimensional variable range hopping. The localization length along the chain is ~50 bond lengths, $\sigma_S$ is the saturation value of $\sigma$.

the Fermi level state density shows a smooth transition through this region). Thus one need not expect a simple correlation between the saturation of the Pauli paramagnetic response and the saturation of the conductivity in this system. The absence of such a correlation is characteristic of the currently available experimental data on this system.

This discussion opens a number of intriguing, unanswered questions. The estimated mobilities in highly doped $(CH)_x$ are uncharacteristically large[47] for a system in which the transport is due to hopping, for instance. A second and not unrelated question is how the characteristic electronic localization length itself varies as a function of concentration. We may expect that the localized states are more delocalized at $c = 0.10$ than $c = 0.03$. Finally the use of the variable-range hopping models is poorly justified if the disorder on the chain is correlated over the length of an average hop, as quite probably occurs in this system. A further speculation worth mentioning is that some remnant of a collective transport mech-

anism occurs in the doping regime over which the distorted charge density wave survives the disorder. Frequency-, temperature-, and electric-field-dependent studies of the conductivity of iodine-doped polyacetylene in the concentration regime which encompasses the insulator-metal transition show that disorder plays a dominant role.[48]

Finally the picture of a closing gap due to disorder seems to be generally consistent with the core level excitation spectroscopy reported by Ritsko[57] which shows a qualitative change of the carbon $K$-edge absorption spectra in highly doped $(CH)_x$ compared with core excitation spectra obtained in pristine $(CH)_x$. The characteristic insulatorlike excitonic edge in pristine spectra is found to be replaced by a rounded featureless edge characteristic of metallic systems in doped samples in these studies.[53]

## VIII. SYNOPSIS

We have discussed a scenario by which highly doped polyacetylene is expected to become metallic. The important elements in this transition are given at the conclusion of Sec. VI. The fundamental picture to emerge from this study is that polyacetylene at an arbitrary doping level within 20% of the half-filled band has a strong intrinsic tendency to seek an *insulating* state. The metallic state occurs when this tendency finally yields to the stronger influence of disorder in the sample due to the added impurities. The persistence of a pseudogap and bond alternation into this metallic state are both evidence of the strong underlying preference of $(CH)_x$ for an insulating ground state. The metallic state which occurs at the insulator-metal "transition" is characterized by a finite density of *localized* states at the Fermi energy. At very high impurity concentrations (>10%) a metallic structure with nearly uniform C–C bond lengths is anticipated. Finally, this transition is not abrupt as it is particularly likely to be smeared by inevitable fluctuations in local dopant density.

## ACKNOWLEDGMENTS

Helpful discussions with J. Bardeen, A. J. Epstein, and D. Vanderbilt are gratefully acknowledged.

[1]H. Shirakawa and S. Ikeda, Polymer J. 2, 231 (1971).
[2]H. Shirakawa, T. Ito, and S. Ikeda, Polymer J. 4, 460 (1973).
[3]C. K. Chiang, C. R. Fincher, Y. W. Park, A. J. Heeger, H. Shirakawa, E. J. Louis, S. C. Gau, and A. G. MacDiarmid, Phys. Rev. Lett. 39, 1098 (1977).
[4]C. K. Chiang, S. C. Gau, C. R. Fincher, Y. W. Park, A. G. MacDiarmid, and A. J. Heeger, Appl. Phys. Lett. 33, 18 (1978).
[5]T. Tani, P. M. Grant, W. D. Gill, G. B. Street, and T. C. Clarke, Solid State Commun. 33, 4991 (1980).
[6]S. Etemad (unpublished).
[7]P. M. Grant and J. P. Batra, Solid State Commun. 29, 225 (1979).
[8]M. Kertesz, J. Koller, and A. Azman, J. Chem. Phys. 67, 1180 (1977).
[9]M. Kertesz, Chem. Phys. 44, 349 (1979).
[10]R. A. Harris and L. M. Falicov, J. Chem. Phys. 51, 5034 (1969).
[11]A. A. Ovchinnikov, I. I. Ukrainskii, and G. V. Kventsel, Usp. Fiz. Nauk 108, 81 (1972) [Sov. Phys.-Uspekhi 15, 575 (1973)].
[12]C. B. Duke, P. Paton, W. R. Salaneck, H. R. Thomas, E. W. Plummer, A. J. Heeger, and A. G. MacDiarmid, Chem. Phys. Lett. 59, 146 (1978).
[13]P. A. Lee, T. M. Rice, and P. W. Anderson; Solid State Commun. 14, 703 (1974), H. Frohlich, Proc. R. Soc. London A223, 296 (1954).
[14]M. J. Rice and S. Strassler, Solid State Commun. 13, 125 (1979).
[15]A. Karpfen and J. Petkov, Solid State Commun. 29, 251 (1979).
[16]G. Beni, Solid State Commun. 15, 269 (1974).
[17]R. E. Peierls, *Quantum Theory of Solids* (Clarendon, Oxford, 1955).
[18]J. Bart and C. H. MacGillavry, Acta Crystallogr. B 24, 1569 (1968).
[19]M. J. Rice, Phys. Lett. 71A, 152 (1979).
[20]W. P. Su, J. R. Schrieffer, and A. J. Heeger, Phys. Rev. Lett. 42, 1698 (1979).
[21]M. J. Rice and E. J. Mele, Solid State Commun. 35, 487 (1980).
[22]W. P. Su and J. R. Schrieffer, Phys. Rev. B 21, 1 (1980).
[23]A. J. Epstein, H. Rommelman, M. Druy, A. J. Heeger, and A. G. MacDiarmid (unpublished).
[24]B. R. Weinberger, J. Kaufer, A. J. Heeger, A. Pron, and A. G. MacDiarmid, Phys. Rev. B 20, 2231 (1979).
[25]C. R. Fincher, M. Ozaki, M. Tanaka, D. Peebles, L. Lauchlan, and A. J. Heeger, Phys. Rev. B 20, 1589 (1979); N. Suzuki, M. Ozaki, S. Etamad, A. J. Heeger, and A. G. MacDiarmid, Phys. Rev. Lett. 45, 1209 (1980); 45, 1463 (1980).
[26]C. R. Fincher, M. Ozaki, A. J. Heeger, and A. G. MacDiarmid, Phys. Rev. B 19, 4140 (1979).
[27]E. J. Mele and M. J. Rice, Phys. Rev. Lett. 45, 926 (1980).
[28]J. Stuke, in *Selenium*, edited by R. A. Zingaro and W. C. Cooper (Van Nostrand Reinhold, New York, 1974), p. 174f.
[29]For a preliminary account of the present work see M. J. Rice and E. J. Mele, Chem. Scr. (in press).

[30]N. F. Mott, *Metal Insulator Transitions* (Taylor and Francis, London, 1974).
[31]D. Vanderbilt and E. J. Mele, Phys. Rev. B 22, 3939 (1980).
[32]W. P. Su, Solid State Commun. 35, 899 (1980).
[33]W. P. Su and J. R. Schreiffer, Proc. Nat. Acad. Sci. (U.S.A.) (in press).
[34]F. Inagaki, M. Tasumi, and T. Miyazawa, J. Raman Spectros. 3, 335 (1975).
[35]E. J. Mele and M. J. Rice, Solid State Commun. 34, 339 (1980).
[36]R. M. Gavin and S. A. Rice, J. Chem. Phys. 55, 1675 (1971).
[37]T. Kakitani, Prog. Theor. Phys. 51, 656 (1974).
[38]D. J. Chadi, Phys. Rev. Lett. 41, 1062 (1978).
[39]D. Vanderbilt and J. D. Joannopoulos, Phys. Rev. B 22, 2927 (1980).
[40]J. D. Joannopoulos and M. L. Cohen, *Solid State Physics* (Academic, New York, 1975), Vol. 31, p. 71.
[41]R. Haydock, Philos. Mag. B 37, 971 (1978).
[42]K. Huang, *Statistical Mechanics* (Wiley, New York, 1963).
[43]M. Abramowitz and I. A. Stegun, *Handbook of Mathematical Functions*, Appl. Math. Series 55 (National Bureau of Standards, Washington, D. C., 1964).
[44]M. J. Rice and J. Timonen, Phys. Lett. 73A, 368 (1979).
[45]H. Fukuyama and P. A. Lee, Phys. Rev. B 17, 535 (1978).
[46]A. Kotani, J. Phys. Soc. Jpn. 42, 416 (1977).
[47]Y. W. Park, Ph.D. thesis, University of Pennsylvania (unpublished); J. F. Kwak, T. C. Clarke, R. L. Greene, and G. B. Street, Solid State Commun. 31, 355 (1979).
[48]A. J. Epstein, H. W. Gibson, P. M. Chaikin, W. G. Clark, and G. Gruner, Phys. Rev. Lett. 45, 1730 (1980); Chem. Scr. (in press).
[49]Y. Tomkiewicz, T. D. Schultz, H. D. Broom, T. C. Clarke, and G. B. Street, Phys. Rev. Lett. 43, 1532 (1979).
[50]R. V. Kasowski, E. Caruthers, and W. Y. Hsu, Phys. Rev. Lett. 44, 676 (1980).
[51]R. H. Baughman, S. L. Hsu, G. P. Pez, and A. J. Signorelli, J. Chem. Phys. 68, 121 (1978).
[52]M. J. Rice and S. Strassler, Solid State Commun. 13, 1389 (1973).
[53]P. A. Lee, T. M. Rice, and P. W. Anderson, Phys. Rev. Lett. 31, 462 (1973).
[54]K. Maki, in *Superconductivity*, edited by R. D. Parks (Marcel Deckzer, New York, 1969), Vol. 2, p. 1035f.
[55]J. J. Ritsko, E. J. Mele, A. J. Heeger, A. G. MacDiarmid, and M. Ozaki, Phys. Rev. Lett. 44, 1351 (1980).
[56]B. Horowitz, Solid State Commun. 34, 611 (1980).
[57]J. J. Ritsko (unpublished).